Supplementary figures

Supplementary figure 1. WD-fed mice are intolerant of high dose IL-23 MC and exhibit gut symptoms

C57BL/6 mice were fed with a WD or an otherwise nutritionally matched control diet (CD) for 6 weeks and then injected with 10 ug IL-23 minicircle DNA (MC). (a) Survival rate after gene delivery. (b) clinical photographs showing loose stool and diarrhea in WD-fed, IL-23 MC-treated mice at day 12 after gene delivery. 8 mice per group.
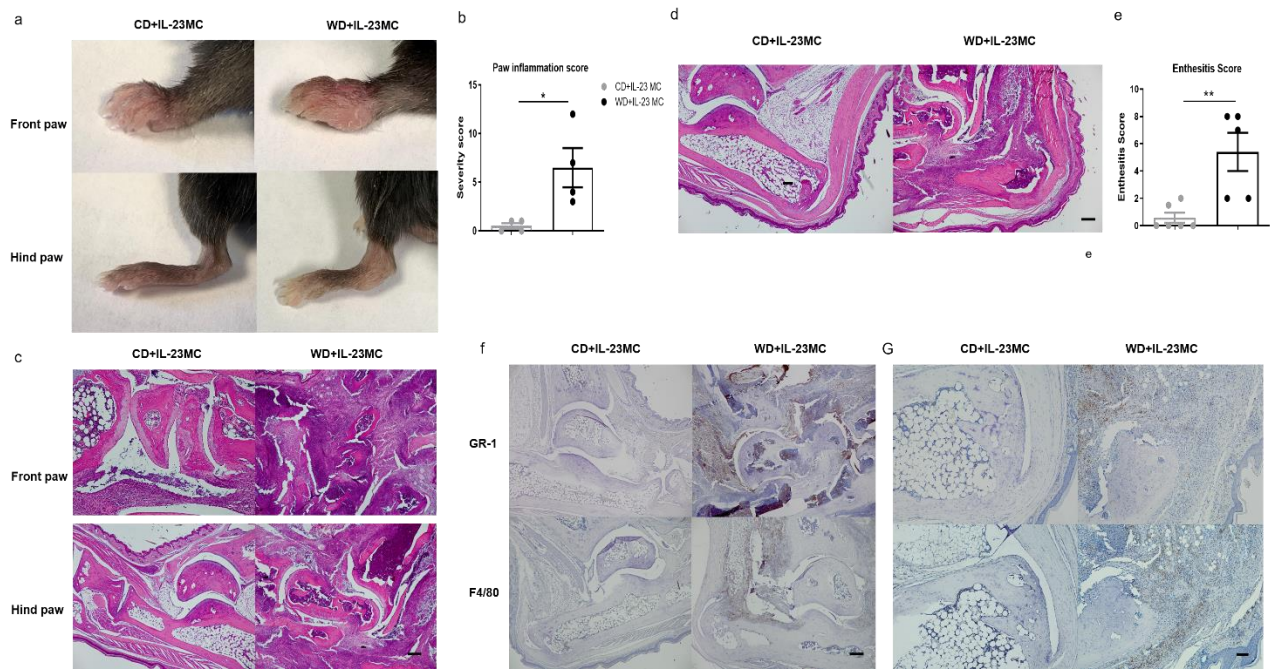
Supplementary figure 2. Exposure to WD enhances susceptibility to IL-23-mediated joint inflammation in B10.RIII mice

B10.RIII mice were fed with a WD or CD for 6 weeks and then injected with 3 µg of IL-23 MC. After MC delivery, mice were maintained on their respective diets for an additional 4 weeks. (a) Clinical photographs showing swollen joints and (b) score of paw inflammation from B10.RIII mice fed with CD or WD after IL-23 MC delivery. (c, d) Representative images of H&E section showing joint inflammation (c) and enthesitis (d) (scale bars, 200 µm). (e) Enthesitis score. (f, g) Representative images of immunohistochemical staining GR-1 and F4/80 in ankle joints (f) and Achilles tendon (g) (scale bars, 100 µm). All of the data are presented as mean± SEM. 4-5 mice per group. Data are representative of two independent experiments. * $p < 0.05$, ** $p < 0.01$, by using Student's T test in (b, d).
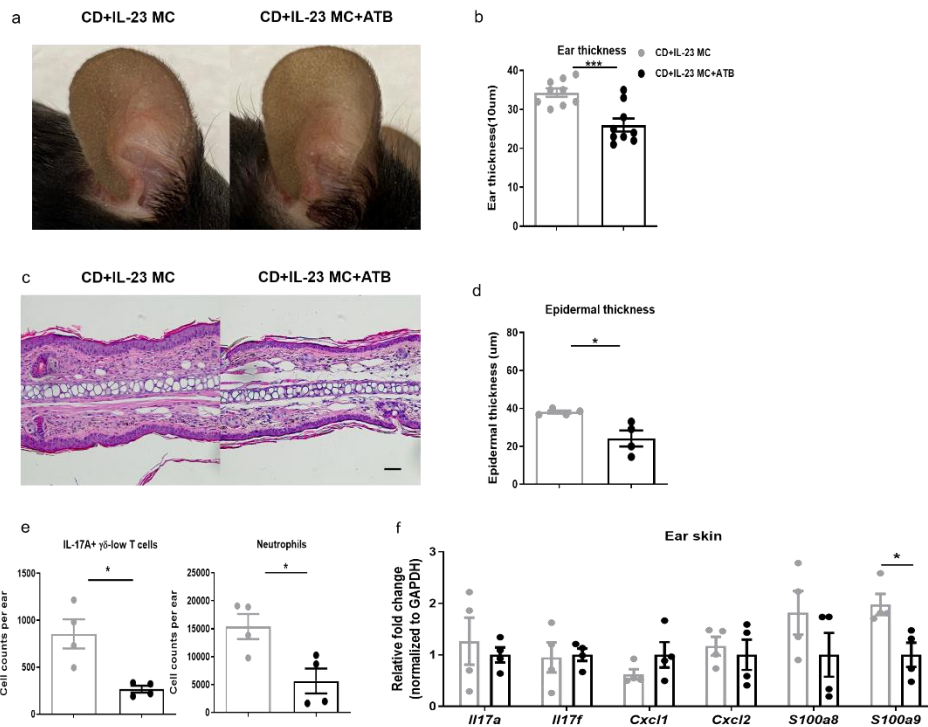
Supplementary figure 3. Antibiotic treatment attenuates IL-23-driven skin inflammation

CD-fed C57BL/6 mice were treated with broad-spectrum combination antibiotics (ATB) or vehicle daily for 6 weeks by oral gavage before IL-23 MC delivery. (a) Representative photographs, (b) ear thickness, (c) image of H&E section (scale bars, 50 μm), (d) histological analysis of epidermal thickness, (e) absolute numbers of IL-17A-producing γδ-low T cells and neutrophils, and (f) gene expression of proinflammatory markers in ear skin. All of the data are presented as mean± SEM. 4 mice per group. Data are representative of two independent experiments. * p <0.05, ** p <0.01. *** p <0.001, by using Student's T test.
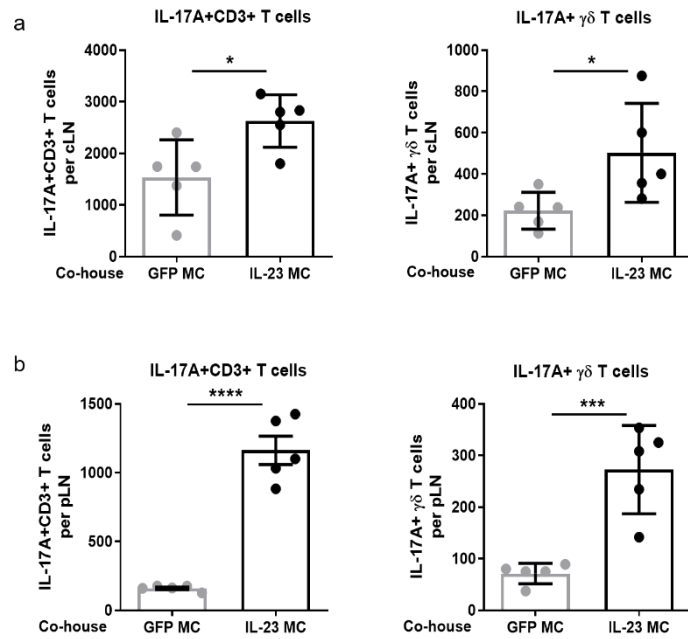
Supplementary figure 4. Co-housing with IL-23 MC-injected mice potentiates IL-17 production by T cell in naïve mice.

Immediately after gene delivery, IL-23 MC or GFP-MC-injected mice were co-housed with naïve mice for 4 weeks. Absolute numbers of IL-17A-producing CD3+ T cell and γδ-low T cells in per (a) cervical lymph node (cLN) or (b) popliteal lymph node (pLN) from naïve mice co-housed with GFP MC or IL-23 MC. All of the data are presented as mean± SEM. 5 mice per group. Data are representative of two independent experiments. * p <0.05, *** p <0.001, **** p <0.0001, by using Student's T test.
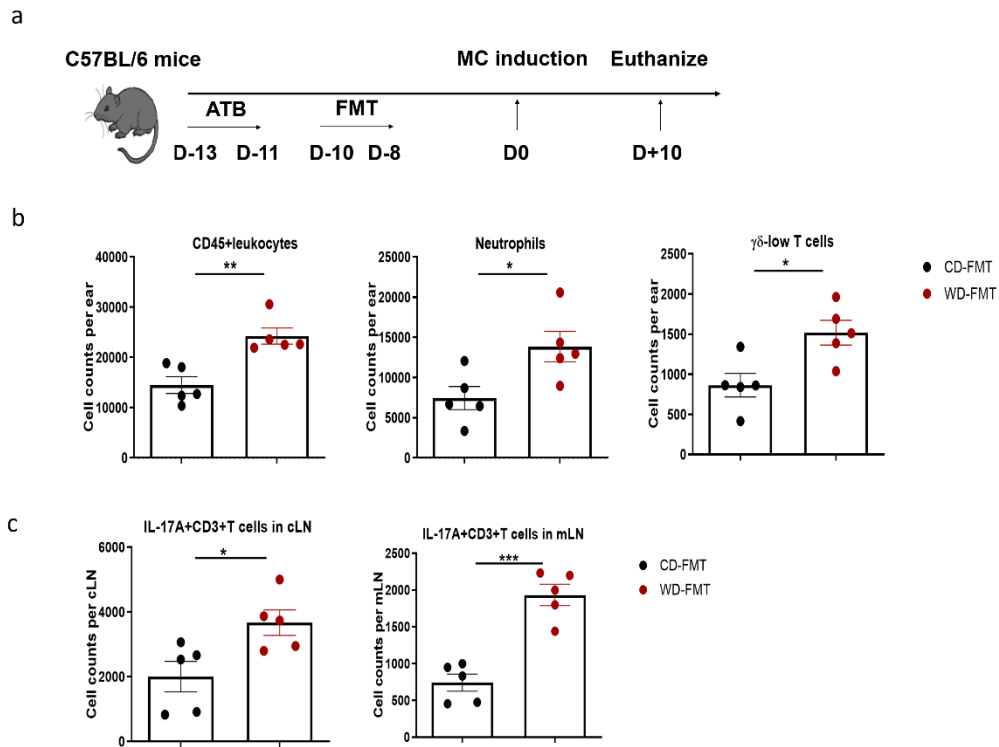
Supplementary figure 5. Fecal microbiota transplantation (FMT) from WD-fed mice promotes inflammatory cellular infiltration in ear skin and draining lymph nodes

(a)Experimental settings of fecal microbiota transplantation: fecal microbiome from CD or WD-fed mice was transplanted into SPF mice after 3 days of ATB treatment. One weeks later, the mice were injected with 5 ug IL-23 MC and euthanized for further analysis at day 10 after MC delivery (B) Absolute numbers of CD45+leukocytes, neutrophils and γδ-low T cells in ear skin. (C) IL-17A-producing CD3+ T cell in per cervical lymph node (cLN) or mesentriclymph node (mLN). All of the data are presented as mean± SEM. 5 mice per group. * p <0.05, ** p <0.01, *** p <0.001, by using Student's T test.
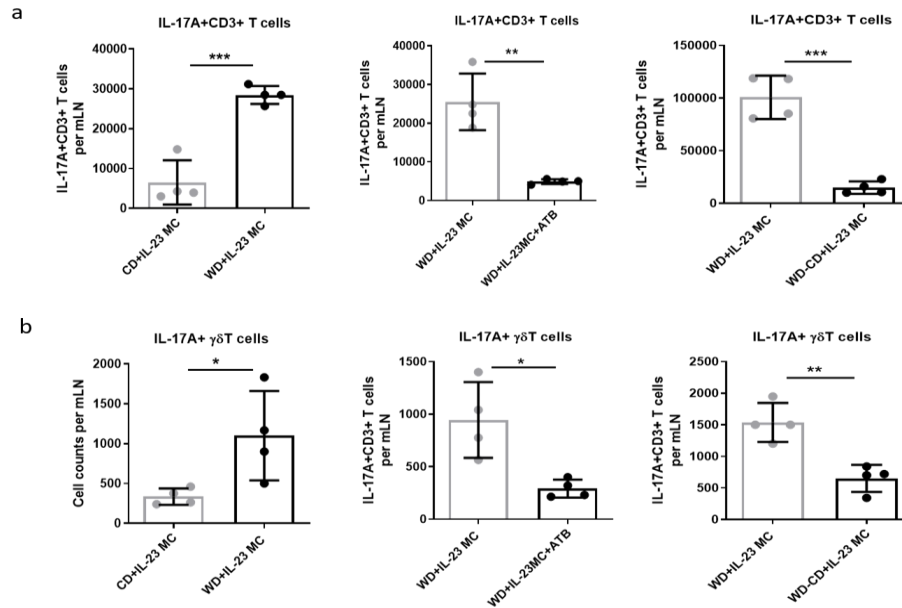
Supplementary figure 6. WD intake is associated with accumulation of IL-17A-producing CD3+ T cells and γδ T cells in the mesenteric lymph nodes (mLN) of IL-23 MC-injected mice

Absolute number of IL-17A-producing CD3+ T cells (a) and γδ T cells (b) in mesenteric lymph nodes (mLN) from CD or WD-fed mice injected with IL-23 MC (right panel), WD-fed, IL-23 MC-injected mice treated with vehicle or with broad coverage antibiotics (ATB) (middle panel), IL-23 MC-injected mice maintained on WD or switched from a WD to a CD. Determined by flow cytometry. * p<0.05, ** p <0.01. *** p <0.001 ,as calculated by two-tailed, unpaired Student's t test

Supplementary table

Table S1.LEfSe analysis showing significant differences in bacterial abundance between CD+GFP MC vs WD+GFP MC

	Group	LDA	p-value
ACTINOBACTERIA			
c_Actinobacteria	CD+GFP MC	-3.3709671	0.0032759
o_Bifidobacteriales	CD+GFP MC	-3.3970199	0.00033107
f_Bifidobacteriaceae	CD+GFP MC	-3.3970201	0.00033107
g_Bifidobacterium	CD+GFP MC	-3.3970199	0.00033107
BACTEROIDETES			
p_Bacteroidetes	CD+GFP MC	-4.4009256	0.00077753
c_Bacteroidia	CD+GFP MC	-4.4009256	0.00077753
o_Bacteroidales	CD+GFP MC	-4.4009256	0.00077753
f_Muribaculaceae	CD+GFP MC	-4.3516401	0.00077753
f_Rikenellaceae	CD+GFP MC	-3.33347	0.01571435
g_Alistipes	CD+GFP MC	-3.33347	0.01571435
FIRMICUTES			
s_Lactobacillus reuteri	CD+GFP MC	-3.3111563	0.02086258
f_Clostridiaceae 1	CD+GFP MC	-3.3952949	0.0004511
g_Lachnospiraceae NK4A136 group	CD+GFP MC	-3.7755973	0.00457444
f_Peptococcaceae	CD+GFP MC	-3.2647202	0.00632295
g_Ruminococcaceae UCG-014	CD+GFP MC	-3.1794801	0.01571435
PROTEOBACTERIA			
c_Gammaproteobacteria	CD+GFP MC	-3.6811039	0.00075005
ACTINOBACTERIA			
c_Coriobacteriia	WD+GFP MC	3.13056093	0.0356919

o_Coriobacteriales	WD+GFP MC	3.13056093	0.0356919
f_Eggerthellaceae	WD+GFP MC	3.13012801	0.0356919
g_Enterorhabdus	WD+GFP MC	3.27402233	0.01171869
BACTEROIDETES			
s_Bacteroides vulgatus	WD+GFP MC	3.3821774	0.00457444
FIRMICUTES			
p_Firmicutes	WD+GFP MC	4.28769996	0.00162919
f_Streptococcaceae	WD+GFP MC	4.05805784	0.00077753
g_Lactococcus	WD+GFP MC	4.06266488	0.00071008
c_Clostridia	WD+GFP MC	4.20571634	0.00632295
o_Clostridiales	WD+GFP MC	4.20571634	0.00632295
g_Blautia	WD+GFP MC	4.02962376	0.00077753
g_Lachnoclostridium	WD+GFP MC	3.36609571	0.00113133
g_Roseburia	WD+GFP MC	3.41777984	0.00113133
f_Peptostreptococcaceae	WD+GFP MC	3.69111219	0.0023221
g_Romboutsia	WD+GFP MC	3.69114943	0.0023221
f_Ruminococcaceae	WD+GFP MC	3.92648243	0.00077753
g_Eubacterium coprostanoligenes group	WD+GFP MC	3.81074759	0.00077753
g_Ruminiclostridium	WD+GFP MC	3.25579245	0.00865154
g_Ruminiclostridium 9	WD+GFP MC	3.2650806	0.0023221
g_Erysipelatoclostridium	WD+GFP MC	3.53736056	0.00077753
PROTEOBACTERIA			
p_Proteobacteria	WD+GFP MC	3.7491649	0.00077753
c_Deltaproteobacteria	WD+GFP MC	3.775532	0.0004511
o_Desulfovibrionales	WD+GFP MC	3.77963286	0.0004511
f_Desulfovibrionaceae	WD+GFP MC	3.77830797	0.0004511
g_Bilophila	WD+GFP MC	3.77496957	0.0004511

Table S2.LEfSe analysis showing significant differences in bacterial abundance between CD+GFP MC vs CD+IL-23 MC

	Group	LDA	p-value
ACTINOBACTERIA			
c_Actinobacteria	CD+GFP MC	-3.4109273	0.00071008
o_Bifidobacteriales	CD+GFP MC	-3.410463	0.00071008
f_Bifidobacteriaceae	CD+GFP MC	-3.410463	0.00071008
g_Bifidobacterium	CD+GFP MC	-3.410463	0.00071008
FIRMICUTES			
g_Lactococcus	CD+GFP MC	-2.6455695	0.02727851
f_Clostridiaceae 1	CD+GFP MC	-3.2792011	0.00033107
f_Peptostreptococcaceae	CD+GFP MC	-2.6354775	0.00119375
g_Romboutsia	CD+GFP MC	-2.634685	0.00119375
VERRUCOMICROBIOTA			
p_Verrucomicrobia	CD+GFP MC	-2.9566109	0.02727851
c_Verrucomicrobiae	CD+GFP MC	-2.9566104	0.02727851
o_Verrucomicrobiales	CD+GFP MC	-2.9566105	0.02727851
f_Akkermansiaceae	CD+GFP MC	-2.9566114	0.02727851
g_Akkermansia	CD+GFP MC	-2.9566113	0.02727851
ACTINOBACTERIA			
c_Coriobacteriia	CD+IL-23 MC	2.47356973	0.01571435
o_Coriobacteriales	CD+IL-23 MC	2.47356973	0.01571435
f_Eggerthellaceae	CD+IL-23 MC	2.47445485	0.01571435
g_Enterorhabdus	CD+IL-23 MC	2.57044068	0.01571435
BACTEROIDETES			
f_Bacteroidaceae	CD+IL-23 MC	3.60438822	0.04599937
g_Bacteroides	CD+IL-23 MC	3.60438822	0.04599937
g_Muribaculum	CD+IL-23 MC	3.42924478	0.00033107

FIRMICUTES			
g_Eubacterium fissicatena group	CD+IL-23 MC	3.35610481	0.01171869
g_Marvinbryantia	CD+IL-23 MC	3.19867631	0.0032759
g_Eubacterium coprostanoligenes group	CD+IL-23 MC	2.83861331	0.02742315
g_Erysipelatoclostridium	CD+IL-23 MC	2.8275634	0.00162919
PROTEOBACTERIA			
g_Escherichia-Shigella	CD+IL-23 MC	2.91170909	0.01065638

Table S3.LEfSe analysis showing significant differences in bacterial abundance between WD+GFP MC vs WD+IL-23 MC

	Group	**LDA**	**p-value**
ACTINOBACTERIA			
p_Actinobacteria	WD+GFP MC	-2.9237788	0.00162919
c_Coriobacteriia	WD+GFP MC	-2.9988012	0.00077753
o_Coriobacteriales	WD+GFP MC	-2.9988012	0.00077753
f_Eggerthellaceae	WD+GFP MC	-2.9993678	0.00077753
g_Enterorhabdus	WD+GFP MC	-2.9993678	0.00077753
BACTEROIDETES			
s_Bacteroides uniformis	WD+GFP MC	-2.7788784	0.01571435
FIRMICUTES			
p_Firmicutes	WD+GFP MC	-4.1345015	0.02086258
f_Streptococcaceae	WD+GFP MC	-3.9622695	0.00162919
g_Lactococcus	WD+GFP MC	-3.9730832	0.00113133
c_Clostridia	WD+GFP MC	-4.4770553	0.00077753
o_Clostridiales	WD+GFP MC	-4.4770553	0.00077753
f_Lachnospiraceae	WD+GFP MC	-4.2426095	0.00162919
g_Blautia	WD+GFP MC	-3.9571942	0.00113133

g_GCA-900066575	WD+GFP MC	-2.8351544	0.01571435
g_Lachnoclostridium	WD+GFP MC	-3.0834075	0.02086258
g_Roseburia	WD+GFP MC	-3.3235807	0.01171869
f_Peptostreptococcaceae	WD+GFP MC	-3.7043471	0.00033107
g_Romboutsia	WD+GFP MC	-3.7043472	0.00033107
f_Ruminococcaceae	WD+GFP MC	-3.8942809	0.00113133
g__Eubacterium coprostanoligenes group	WD+GFP MC	-3.6369589	0.00077753
g_Ruminiclostridium	WD+GFP MC	-2.9143861	0.04599937
g_Ruminiclostridium 9	WD+GFP MC	-3.0519789	0.0023221
PROTEOBACTERIA			
c_Deltaproteobacteria	WD+GFP MC	-3.6301281	0.0007706
o_Desulfovibrionales	WD+GFP MC	-3.6301281	0.0007706
f_Desulfovibrionaceae	WD+GFP MC	-3.6301281	0.0007706
g_Bilophila	WD+GFP MC	-3.6301281	0.0007706
ACTINOBACTERIA			
o_Bifidobacteriales	WD+IL-23 MC	2.75585155	0.02727851
f_Bifidobacteriaceae	WD+IL-23 MC	2.75585085	0.02727851
g_Bifidobacterium	WD+IL-23 MC	2.75585835	0.02727851
BACTEROIDETES			
g_Muribaculum	WD+IL-23 MC	2.98171199	0.00119375
FIRMICUTES			
f_Lactobacillaceae	WD+IL-23 MC	4.36160915	0.0023221
g_Lactobacillus	WD+IL-23 MC	4.36160915	0.0023221
s_Lactobacillus johnsonii	WD+IL-23 MC	4.2429784	0.00113133
s_Lactobacillus reuteri	WD+IL-23 MC	3.64555757	0.00077753
PROTEOBACTERIA			
c_Gammaproteobacteria	WD+IL-23 MC	3.45878598	0.00845642
o_Enterobacteriales	WD+IL-23 MC	3.39775424	0.00138379

	Group	LDA	p-value
f_Enterobacteriaceae	WD+IL-23 MC	3.39770803	0.00138379
g_Escherichia-Shigella	WD+IL-23 MC	3.39590036	0.00138379
VERRUCOMICROBIA			
p_Verrucomicrobia	WD+IL-23 MC	3.8128162	0.01359026
c_Verrucomicrobiae	WD+IL-23 MC	3.81281372	0.01359026
o_Verrucomicrobiales	WD+IL-23 MC	3.8126245	0.01359026
f_Akkermansiaceae	WD+IL-23 MC	3.8128661	0.01359026
g_Akkermansia	WD+IL-23 MC	3.81270656	0.01359026

Table S4.LEfSe analysis showing significant differences in bacterial abundance between CD+IL-23 MC vs WD+IL-23 MC

	Group	LDA	p-value
ACTINOBACTERIA			
p_Actinobacteria	CD+IL-23 MC	-3.1644044	0.0032759
c_Coriobacteriia	CD+IL-23 MC	-3.2227457	0.00077753
o_Coriobacteriales	CD+IL-23 MC	-3.2227457	0.00077753
f_Eggerthellaceae	CD+IL-23 MC	-3.2250688	0.00077753
g_Enterorhabdus	CD+IL-23 MC	-3.3535624	0.00077753
BACTEROIDETES			
p_Bacteroidetes	CD+IL-23 MC	-4.3183134	0.00077753
c_Bacteroidia	CD+IL-23 MC	-4.3183134	0.00077753
o_Bacteroidales	CD+IL-23 MC	-4.3183134	0.00077753
s_Bacteroides uniformis	CD+IL-23 MC	-3.1796248	0.02742315
f_Muribaculaceae	CD+IL-23 MC	-4.2766478	0.00077753
g_Muribaculum	CD+IL-23 MC	-3.3164794	0.00457444
FIRMICUTES			
c_Clostridia	CD+IL-23 MC	-4.0332464	0.02086258
o_Clostridiales	CD+IL-23 MC	-4.0332464	0.02086258
f_Lachnospiraceae	CD+IL-23 MC	-4.0459742	0.01571435

g_Lachnospiraceae NK4A136 group	CD+IL-23 MC	-3.8612131	0.00457444
g_Marvinbryantia	CD+IL-23 MC	-3.3065505	0.00632295
f_Peptococcaceae	CD+IL-23 MC	-2.8473479	0.02742315
g_Ruminococcaceae UCG-014	CD+IL-23 MC	-3.2407539	0.0016163
FIRMICUTES			
p_Firmicutes	WD+IL-23 MC	3.88873566	0.0356919
p_Firmicutes.c_Bacilli	WD+IL-23 MC	4.22438416	0.02086258
o_Lactobacillales	WD+IL-23 MC	4.22422884	0.02086258
f_Lactobacillaceae	WD+IL-23 MC	4.15199303	0.02742315
g_Lactobacillus	WD+IL-23 MC	4.15199303	0.02742315
ps_Lactobacillus johnsonii	WD+IL-23 MC	4.1659165	0.0032759
s_Lactobacillus reuteri	WD+IL-23 MC	3.38202644	0.0032759
f_Streptococcaceae	WD+IL-23 MC	3.38551607	0.00077753
g_Lactococcus	WD+IL-23 MC	3.36078742	0.00033107
g_Eubacterium coprostanoligenes group	WD+IL-23 MC	3.21631479	0.01571435
g_Ruminiclostridium	WD+IL-23 MC	3.16956133	0.00865154
PROTEOBACTERIA			
c_Deltaproteobacteria	WD+IL-23 MC	3.07346608	0.00777396
o_Desulfovibrionales	WD+IL-23 MC	3.07346012	0.00777396
p_f_Desulfovibrionaceae	WD+IL-23 MC	3.07346056	0.00777396
g_Bilophila	WD+IL-23 MC	3.07346539	0.00777396
o_Enterobacteriales	WD+IL-23 MC	3.33757117	0.0061699
f_Enterobacteriaceae	WD+IL-23 MC	3.33757117	0.0061699
g_Escherichia-Shigella	WD+IL-23 MC	3.33647703	0.0061699
VERRUCOMICROBIA			
p_Verrucomicrobia	WD+IL-23 MC	3.78326837	0.00377634

	Group	LDA	p-value
c_Verrucomicrobiae	WD+IL-23 MC	3.7832684	0.00377634
o_Verrucomicrobiales	WD+IL-23 MC	3.78326838	0.00377634
f_Akkermansiaceae	WD+IL-23 MC	3.78326812	0.00377634
g_Akkermansia	WD+IL-23 MC	3.78326836	0.00377634

Table S5.LEfSe analysis showing significant differences in bacterial abundance between mice maintained on WD or changed to CD

	Group	LDA	p-value
FIRMICUTES			
f_Enterococcaceae	WD+IL-23 MC	-3.4235587	0.01796048
g_Enterococcus	WD+IL-23 MC	-3.4149562	0.01796048
f_Streptococcaceae	WD+IL-23 MC	-3.3316662	0.02092134
g_Lactococcus	WD+IL-23 MC	-3.3037131	0.01387441
f_Peptostreptococcaceae	WD+IL-23 MC	-3.7231472	0.0472209
g_Terrisporobacter	WD+IL-23 MC	-3.6841821	0.0472209
PROTEOBACTERIA			
p_Proteobacteria	WD+IL-23 MC	-4.1895841	0.04330814
g_Proteus	WD+IL-23 MC	-3.1217528	0.0472209
ACTINOBACTERIA			
p_Actinobacteria	WD-CD+IL-23 MC	3.04115681	0.04330814
c_Coriobacteriia	WD-CD+IL-23 MC	3.22580609	0.01796048
o_Coriobacteriales	WD-CD+IL-23 MC	3.27132947	0.01796048
f_Eggerthellaceae	WD-CD+IL-23 MC	3.2607899	0.01796048
g_Enterorhabdus	WD-CD+IL-23 MC	3.19431696	0.01796048
BACTEROIDETES			
p_Bacteroidetes	WD-CD+IL-23 MC	4.19687782	0.02092134
c_Bacteroidia	WD-CD+IL-23 MC	4.22877569	0.02092134
o_Bacteroidales	WD-CD+IL-23 MC	4.21918187	0.02092134

f_Muribaculaceae	WD-CD+IL-23 MC	4.12112275	0.01796048
g_Muribaculum	WD-CD+IL-23 MC	3.25353442	0.01796048
f_Rikenellaceae	WD-CD+IL-23 MC	3.24143461	0.01796048
g_Alistipes	WD-CD+IL-23 MC	3.24826259	0.01796048
FITMICUTES			
c_Erysipelotrichia	WD-CD+IL-23 MC	3.02895531	0.04330814
o_Erysipelotrichales	WD-CD+IL-23 MC	2.97466396	0.04330814
f_Erysipelotrichaceae	WD-CD+IL-23 MC	3.00226158	0.04330814
g_Erysipelatoclostridium	WD-CD+IL-23 MC	3.20046775	0.01796048

Supplementary methods

Mice

C57BL/6 mice or B10.RIII-H2r H2-T18b/(71NS)SnJ (B10.RIII) were purchased from The Jackson Laboratory (Bar Harbor, ME) and used in institutionally approved animal protocols (University of California, Davis). Mice with different treatment were not co-housed unless stated otherwise. Mice within a treatment group were distributed across multiple cages to reduce cage effects.

Production and purification of GFP and IL-23 minicircle (MC) DNA and hydrodynamic delivery

Minicircle-RSV.Flag.mIL23.elasti.bpA or RSV.eGFP.bpA was produced as described (Chen et al., 2005). To produce minicircle-RSV.Flag.mIL23.elasti.bpA or RSV.eGFP.bpA, a single isolated colony from a fresh plate was grown for 8 h in 2 ml of Luria–Bertani broth with kanamycin. Eight hundred microliters of this culture was used to inoculate 1 L of Terrific broth and grown for an additional 17 h. Overnight, cultures were centrifuged at 20°C, 4000 rpm for 20 min. The pellet was resuspended at 4:1 (v/v) in fresh Luria–Bertani broth containing 1% L-arabinose. The bacteria were incubated at 32°C with constant shaking at 220 rpm for 2 h. After adding half volume of fresh low-salt Luria–Bertani broth (pH 8.0) containing 1% L-arabinose, the incubation temperature was increased to 37°C and the incubation was continued for an additional 2h. Episomal DNA minicircles (MC) were prepared from bacteria using EndoFree Megaprep plasmid purification kits from Qiagen (Chatsworth, CA)

according to the manual instruction.

Hydrodynamic delivery of IL-23 or GFP MC DNA via tail vein injection was performed as previously described (Adamopoulos et al., 2011). MC was prepared in lactated ringers solution and administrated by hydrodynamic delivery into the tail vein. Mice were mechanically restrained and received a volume of 10% bodyweight within a period of 5–7 s. Serum IL-23 was assayed using an ELISA kit purchased from Invitrogen (Waltham, MA) in accordance with the manufacturer's instructions.

The IL-23 minicircle (MC)-based murine model has several advantages: first, hydrodynamic delivery of IL-23 MC results in persistent, high-level of IL-23 gene expression and induces strong phenotype of psoriatic inflammation over 2 months, thus providing enough window period to test the influence of diet (or change of diet pattern) on established disease; second, this model developed concurrent skin and joint changes that have some of the features found in human psoriatic skin and joints, allowing us to study the two major sequellae of psoriasis, PsD and PsA, at the same time; moreover, contrast to other transgenic mice models, we can easily modify the degree of the inflammation by tittering the dose of MC.

However this model is dominated by IL-23/IL-17A axis, it may have limitations in studying other pathways like TNFα.

Sample preparation for flow cytometry

Anti–mouse γδ-TCR (clone GL3), CD45 (30-F11), CD3(17A2),CCR6 (29-2L17), CD11b (M1/70), Ly6G (IA8) antibodies were purchased from BioLegend (San Diego,

CA). Anti–IL-17A (eBio17B7) antibody was purchased from eBioscience (San Diego, CA). Whole ear skin was minced and digested with Liberase TM (Roche, Mannheim) and DNase I (Sigma-Aldrich) with addition of 5% fetal bovine serum to obtain whole skin cell suspensions before passing tissue through a 70-um cell strainer. Single-cell suspensions from the cervical draining or popliteal lymph nodes were prepared by mashing the tissue through a 70-um cell strainer. Intracellular staining was done after incubating cells for 2 hours with cell stimulation cocktail (eBioscience). Anti-mouse CD16/32 (BD Biosciences, San Jose, CA) was added to cells prior to staining to block binding to Fc-receptors.

Evaluation of joints and enthesitis with disease scoring

Disease severity for each limb was recorded as described before (Bouchareychas et al., 2017): 0, normal; 1, erythema and swelling of one digit; 2, erythema and swelling of two digits; 3, erythema and swelling of more than two digits and/or swelling of an ankle joint. The clinical arthritis score is defined as the sum of the scores for all four paws of each mouse.

Achilles tendon enthesitis was scored on three parameters (Jacques et al., 2014): infiltrate in the Achilles tendon, calcaneal erosion, and exudate at the synovio–entheseal complex. Each parameter was graded on a scale of 0-3, where 0=normal; 1=mild; 2=moderate and 3=severe. The maximum composite score for Achilles tendon enthesitis was 9.

Histopathological analysis and immunohistochemistry (IHC)

Formaldehyde-fixed, paraffin-embedded ear skin samples were stained with H&E using standard procedures. The paw tissue was decalcified with 4% formic acid before embedding. Images were acquired using a Nikon Optiphot 2 microscope (Nikon, Tokyo, Japan). Epidermal thickness was measured with a computer-assisted quantitative image analysis software (ImageJ).

For immunohistochemical analysis, skin sections were incubated with primary antibodies against murine Ki-67, p-stat3, Gr-1, F4/80, followed by the appropriate secondary antibodies. Rinsed sections were counterstained with hematoxylin.

Quantitative real-time PCR

Total RNA of mouse ear skin was extracted using a RNeasy Fibrous Tissue Kit (Qiagen, Hilden, Germany). For paw tissue, the skin was removed from the hind paw before further extraction. Quantitative real-time PCR was performed using Quant Studio 3 real-time PCR system (Applied Biosystems, Foster City, CA). The primers were obtained from Integrated DNA Technologies, Inc (Skokie, IL). The following primers were pre-designed (otherwise the sequence are shown) and obtained from Integrated DNA Technologies, Inc (Skokie, IL, USA):

Gene name	Identifer or sequence
Gapdh	Mm.PT.39a.1
Il17a	Mm.PT.58.6531092),
Il17f	Mm.PT.58.9739903),
Cxcl1	Mm.PT.58.42076891
Cxcl2	Mm.PT.58.10456839
S100a8	Mm.PT.58.44003402

S100a9	Mm.PT.58.41787562
Il1b	Mm.PT.58.41616450
Il6	Mm.PT.58.10005566
Tnf	Mm.PT.58.12575861
Tnfsf11	Mm.PT.58.29202697
Tnfrsf11b	Mm.PT.58.41494681

Antibiotic Treatment

Mice were given oral gavage of antibiotics (ATB-treated group) or water

(vehicle-treated group) on a daily basis throughout the duration of the experiment.

The antibiotic cocktail was comprised of four antibiotics and ampicillin (100 mg/kg),

vancomycin (50 mg/kg), metronidazole (100 mg/kg), neomycin (100 mg/kg),

amphotericin B (1 mg/kg, Amresco Inc). Amphotericin B was added to prevent fungal

overgrowth or opportunistic infections.

Sequencing of microbial communities

DNA was isolated using the Qiagen DNeasy PowerSoil Pro kit (Qiagen) with the

following modification: After addition of buffer CD1, samples were incubated at 65°C

for 10 minutes and then subjected to homogenization using a Biospec

Mini-Beadbeater (Biospec Products) for 2 minutes. Samples were eluted in 100 ul of

buffer C6. Primers 341F (TCGTCGGCAGCGTCAGATGTGTATAAGAGACAG

(spacer) TGCCTACGGGNGGCWGCAG) and 806R

(GTCTCGTGGGCTCGGAGATGT-GTATAAGAGACAG (spacer)

CCGGACTACNVGGGTWTCTAAT) were used to amplify the V3-V4 domain of the

16S rRNA using a two-step PCR procedure. In step one of the amplification procedure, both forward and reverse primers contained an Illumina tag sequence (bold), a variable length spacer (no spacer, A, CA, or GCA for 341F; no spacer, G, TG, ATG for 806R) to increase diversity and improve the quality of the sequencing run, a linker sequence (italicized), and the 16S target sequence (underlined). Each 25 ml PCR reaction contained 1 Unit Kapa2G Robust Hot Start Polymerase (Kapa Biosystems), 1.5 mM MgCl2, 0.2 mM final concentration dNTP mix, 0.2 mM final concentration of each primer, and 1ul of DNA for each sample. PCR conditions were: an initial incubation at 95°C for 3 min, followed by 25 cycles of 95°C for 45 s, 50°C for 30 s, 72°C for 30 s and a final extension of 72°C for 3 min. In step two, each sample was barcoded with a unique forward and reverse barcode combination using forward primers (AATGATACGGCGACCACCGAGATCTA-CACNNNNNNNNT-CGTCGGCAGC GTC) with an Illumina P5 adapter sequence (bold), a unique 8 nt barcode (N), a partial matching sequence of the forward adapter used in step one (underlined), and reverse primers (CAAGCAGAAGACGGCATA-CGAGATNNNN-NNNNGTCTCGTGGGCTCGG) with an Illumina P7 adapter sequence (bold), unique 8 nt barcode (N), and a partial matching sequence of the reverse adapter used in step one (underlined). The PCR reaction in step two contained 1 Unit Kapa2G Robust Hot Start Polymerase (Kapa Biosystems), 1.5 mM MgCl2, 0.2 mM final concentration dNTP mix, 0.2 mM final concentration of each uniquely barcoded primer, and 1ul of the product from the PCR

reaction in step one diluted at a 10:1 ratio in water. PCR conditions were: an initial

incubation at 95°C for 3 min, followed by 9 cycles of 95°C for 30 s, 58°C for 30 s, 72°

C for 30 s and a final extension of 72°C for 3 min.

The final product was quantified on the Qubit instrument using the Qubit High

Sensitivity dsDNA kit (Invitrogen), and individual amplicons were pooled in equal

concentrations. The pooled library was cleaned utilizing Ampure XP beads (Beckman

Coulter) then checked for quality and proper amplicon size on an Agilent 2100

Bioanalyzer (Agilent Technologies). The library was quantified via qPCR followed

by 300-bp paired-end sequencing using an Illumina MiSeq instrument (Illumina) in

the Genome Center DNA Technologies Core, University of California, Davis. DNA

extractions and library preparation were performed by the UC Davis Host Microbe

Systems Biology Core Facility.

Bioinformatics

Demultiplexing of the raw FASTQ files and adapter trimming of sequences were

performed using dbcAmplicons version 0.8.5.

(https://github.com/msettles/dbcAmplicons). Each sequence was assigned to its given

sample based on the given forward and reverse barcode. Reads that did not match any

barcode were discarded (failed to meet minimum quality thresholds). The unmerged

forward and reverse reads were imported into QIIME2 version 2020.2

(https://qiime2.org), and sequence variants were determined following the DADA2

analysis pipeline. Sequences that were only observed one time or only in a single

sample were discarded and chimeras were detected and filtered from paired-end reads. After quality filtering, sequences were clustered into amplicon sequence variants (ASVs). Comparison of clustered sequences were performed and taxonomic classification was assigned using a Naive Bayes filtered classifier trained on the 99% identity SILVA database, version 132. Principal Coordinates Analysis (PCoA) and alpha diversity analysis were performed using the Phyloseq R package (https://doi.org/10.1371/journal.pone.0061217) (unrarified reads). To identify differentially abundant taxa among groups LEfSe analysis were performed using the galaxy web application (http://huttenhower.sph.harvard.edu/galaxy/). Differences between groups were considered significant when the logarithmic LDA score was >2.0 and the p value was <0.05.

Fecal microbiota transplantation (FMT)

The endogenous intestinal microbiota of 8-week old SPF mice was depleted by gavage with broad-spectrum antibiotics for 3 days. The antibiotic cocktail was comprised of four antibiotics, including ampicillin (100 mg/kg), vancomycin (50 mg/kg), metronidazole (100 mg/kg) and neomycin (100 mg/kg) as described (Zhang et al., 2020). The recipient mice were maintained on chow diet throughout the whole experiment. Fresh murine fecal samples were collected directly from the rectums of age- and sex-matched donor mice fed with WD or CD for 6 weeks. The pooled feces were resuspended in sterile PBS (1 mL of PBS/0.2 g of fecal pellet, about 10–12 fecal pellets), homogenized completely with beads and vortex 3x for 1

min each. Homogenates were centrifuged at 800 x g for 3 min and then filtered the by passing through a 70 μm cell strainer. 200 μL of prepared fecal fluid was administered to the microbiota-depleted mice via oral gavage once a day for 3 days.

Statistical analysis

All data are shown as mean ± SEM. Data were analyzed using GraphPad Prism version 6 (GraphPad Software, San Diego, CA). A two-sided unpaired Student's t-test was used to compare two groups, and one-way analysis of variance (ANOVA) Bonferroni post hoc test was used for multiple comparisons unless stated otherwise. The significance of PCoA was assessed by Permanova Test with p value corrected for multiple testing using the Bonferroni method. A p-value less than 0.05 was considered statistically significant.

Reference

Adamopoulos IE, Tessmer M, Chao CC, Adda S, Gorman D, Petro M, et al. IL-23 is critical for induction of arthritis, osteoclast formation, and maintenance of bone mass. J Immunol 2011;187(2):951-9.

Bouchareychas L, Grossinger EM, Kang M, Qiu H, Adamopoulos IE. Critical Role of LTB4/BLT1 in IL-23-Induced Synovial Inflammation and Osteoclastogenesis via NF-kappaB. J Immunol 2017;198(1):452-60.

Chen ZY, He CY, Kay MA. Improved production and purification of minicircle DNA vector free of plasmid bacterial sequences and capable of persistent transgene expression in vivo. Hum Gene Ther 2005;16(1):126-31.

Jacques P, Lambrecht S, Verheugen E, Pauwels E, Kollias G, Armaka M, et al. Proof of concept: enthesitis and new bone formation in spondyloarthritis are driven by mechanical strain and stromal cells. Ann Rheum Dis 2014;73(2):437-45.

Zhang Q, Lu Q, Luo Y. Fecal Microbiota Transplantation and Detection of Prevalence of IgA-Coated Bacteria in the Gut. J Vis Exp 2020(161).